JOURNAL OF AGRICULTURAL AND FOOD CHEMISTRY

Article

pubs.acs.org/JAFC

Micro-nanopores Fabricated by High-Energy Electron Beam Irradiation: Suitable Structure for Controlling Pesticide Loss

Yubin Xiang,[†,‡] Ning Wang,[†,§] Jimei Song,[‡] Dongqing Cai,*[,†,§] and Zhengyan Wu*[,†,§]

[†]Key Laboratory of Ion Beam Bioengineering, Hefei Institutes of Physical Science, Chinese Academy of Sciences, Hefei 230031, People's Republic of China

[‡]School of Chemistry and Chemical Engineering, Anhui University, Hefei 230039, People's Republic of China

[§]Bioenergy Forest Research Center of State Forestry Administration, Hefei 230031, People's Republic of China

ABSTRACT: Pesticide sprayed onto crop leaves tends to be washed off by rainwater and discharge into the environment through leaching and runoff, resulting in severe pollution to both soil and water. Here, to control pesticide loss, we developed a loss-control pesticide (LCP) by adding modified natural nanoclay (diatomite) through high-energy electron beam (HEEB) to traditional pesticide. After HEEB treatment, the originally clogged pores in diatomite opened, resulting in plenty of micro-nanopores in diatomite, which are beneficial for the pesticide molecules to access and be adsorbed. This pesticide-diatomite complex tended to be retained by the rough surface of crop leaves, displaying a high adhesion performance onto the leaves, so that the pesticide loss reduced, sufficient pesticide for crops was supplied, and the pollution risk of the pesticide could be substantially lowered.

KEYWORDS: *Loss-control pesticide, diatomite, high-energy electron beam, micro-nanopore, chlorpyrifos*

INTRODUCTION

Pesticide has been playing an important role in modern agriculture, providing substantial agronomic and economic benefits. However, it has also posed environmental problems because of the loss resulting from leaching and surface runoff, which can cause soil and groundwater contamination. To compensate for the loss and to ensure adequate pest control for a suitable period, pesticides are applied at concentrations greatly exceeding those required for control of the target organisms, thus increasing the likelihood of runoff and leaching and, hence, the risk of surface and groundwater contamination.[1] Such situations may become worse when it rains after pesticide is applied. Therefore, an advanced pesticide with a low loss ratio should be developed.

During the past 30 years, various types of slow release pesticide formulations were developed through encapsulating,[2] microcapsule,[3] tablets,[4,5] etc., using polymers, clays, etc. Although they could effectively enhance pesticide use efficiency, the released unused pesticide tends to be transferred into environment through runoff and leaching. Hence, we believe that controlling pesticide loss is a fundamental and promising countermeasure to reduce the environmental risk of pesticide. It is necessary to develop a new kind of pesticide with advantages of high adhesion capacity on the leaf, low loss amount, long efficacy duration, and thus, low dosage, to decrease the risk of environmental pollution, save the manpower and energy by reducing the number of pesticide applications required, increase the safety for the pesticide applicator, and decrease the non-target effects in comparison to conventional pesticide. In this paper, we reported the development of a new kind of pesticide named loss-control pesticide (LCP) though adding an appropriate amount of diatomite modified by high-energy electron beam (HEEB).

Diatomite is a kind of pale-colored natural clay composed mainly of silica microfossils of aquatic unicellular algae. It consists of a great number of diatom units (DU) with various shapes and sizes (10−200 μm), as well as high porosity (60−90%).[6,7] Because of the high porosity, low density, and high specific surface area, diatomite has been widely applied as filtration media, adsorbent, and catalyst support.[8] With the deepening mining, it is becoming harder to obtain high-quality diatomites and most of the diatomites mined own a high-impurity amount and improper pore size distribution (PSD), because the diatomite pores tend to be clogged with these impurities, which are unfavorable for its application. Hence, it is important to improve the properties of diatomite, including impurity content and PSD, which are the dominant factors for its adsorption and carrier performance. Herein, diatomite was modified using HEEB irradiation to remove the impurities in the diatomite pores and improve the PSD of diatomite; thus, more pesticide could be adsorbed onto diatomite.

Chlorpyrifos [CPF, *O*,*O*-diethyl *O*-(3,5,6-trichloro-2-pyridyl)-phosphorothioate], a broad-spectrum organophosphorus insecticide, is selected as the model pesticide herein, because of its wide application for controlling rice thrips, gall midge, planthoppers, rice leafhopper, termites, etc.[9−14] and the potential adverse impact on the ecosystem or human health. The objective of this work is to develop a new pesticide named loss-control chlorpyrifos (LCC) using HEEB-modified diatomite (HMD) and investigate the adhesion performance of LCC on crop leaves as well as the migration performance in the soil, in comparison to that of CPF with natural diatomite (ND) and

Received: March 20, 2013
Revised: May 13, 2013
Accepted: May 14, 2013
Published: May 14, 2013

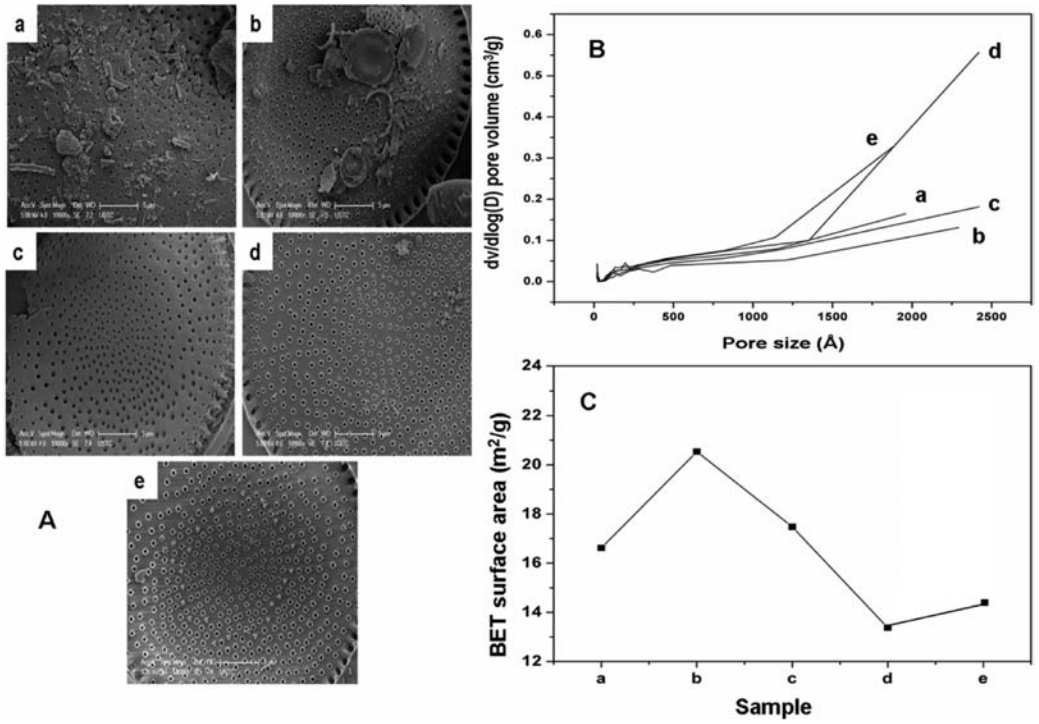

Figure 1. (A) Morphology, (B) PSD, and (C) BET surface area of (a) ND, (b) HMD10, (c) HMD20, (d) HMD30, and (e) HMD40.

CPF alone. It was proven that HMD exhibited an outstanding performance, significantly improving the adhesion ability of CPF. This work may provide a promising method to control pesticide loss and reduce the pollution risk to the environment.

MATERIALS AND METHODS

Materials. The diatomite powder, with an average particle size of 10 μm, was provided by Aobao Co., Ltd. (Shandong, China). CPF with a purity of 99% was provided by Jinghong Chemical Co., Ltd. (Jiangsu, China). Other chemicals were of analytical reagent grade and purchased from Sinopharm Chemical Reagent Company (Shanghai, China). The deionized water was used throughout this work.

HEEB Irradiation. HEEB irradiation of diatomite samples in plastic bags was carried out using the HEEB accelerator (10 MeV and 10 kW) with fluences of 10, 20, 30, and 40 kGy at room temperature, and the samples were designated as HMD10, HMD20, HMD30, and HMD40, respectively.

LCC Emulsion Preparation. A total of 1.0 g of CPF was dissolved in 20 mL of petroleum ether, and then 1 mL of Tween 80 was added to the system. Afterward, 1 mL of the resulting solution was added to 40 mL of deionized water to obtain the CPF emulsion. A total of 0.1 g of HMD (HMD10, HMD20, HMD30, or HMD40) was added to 40 mL of CPF emulsion to make the LCC emulsion, and the resulting samples were designated as CPF10, CPF20, CPF30, and CPF40, respectively. Meanwhile, 0.1 g of ND was also added to 40 mL of CPF emulsion as a control, and the sample was designated as CPF0.

Adhesion Performance Investigation. LCC emulsion (approximately 1 mL) was sprayed (approximately 1 mL/s) evenly onto each peanut leaf, which lay on a Petri dish with a tilt angle of 30° from the ground at 30 °C. Then, deionized water (approximately 5 mL) was sprayed (approximately 1 mL/s) evenly onto each of the resulting peanut leaves to simulate the rainwater. After air-drying, the leaf was put into 10 mL of petroleum ether and shaken for 10 min at 120 rpm to extract the remaining CPF from the leaf surface to the petroleum ether solution, wherein the concentration of CPF was determined thereafter.

Leaching Behavior Investigation. A total of 2.5 g of soil (150–200 mesh) was put into a centrifuge tube (2.5 mL), wherein a hole (diameter of 2 mm) was opened at the bottom, with a little cotton below the soil layer to prevent the soil from leaching out. A total of 3 mL of LCC emulsion was added dropwise to the top of the soil layer. The leachate was collected and extracted with 6 mL of petroleum ether, wherein the concentration of CPF was measured afterward.

Characterization. The morphology and microstructure of diatomite were observed on scanning electron microscopy (SEM) (Sirion 200, FEI Co., Hillsboro, OR). The PSD of diatomite was measured using a porosimetry analyzer (Tristar II, 3020M, Micromeritics, Norcross, GA). The structure and interaction were analyzed using a TTR-III X-ray diffractometer (Rigaku Co., Japan) and a Fourier transform infrared (FTIR) spectrometer (Bruker Co., Germany). The concentration of CPF in the petroleum ether was measured using an ultraviolet-visible (UV-vis) spectrophotometer (UV 2550, Shimadzu Co., Japan) at a wavelength of 293 nm.[15]

RESULTS AND DISCUSSION

Morphology and Microstructure Modification Investigation. Diatomite consisted of mainly amorphous silica and several kinds of organic and inorganic impurities, such as ferric oxide, alumina, etc., which usually existed in the pores of ND, clogging the pores, and thus, the pore size decreased (panel a of Figure 1A), which was unfavorable to its adsorption capacity. Consequently, it is essential to dredge the clogged pores and increase the pore size for the improvement of the adsorption performance of diatomite. Because of the etching and thermal effect of HEEB as well as the oxidation or reduction effect of the free radicals ($O^{\bullet}$, $O_2^{\bullet}$, $OH^{\bullet}$, $H^{\bullet}$, etc.) formed in the irradiation process, plenty of organic impurities could be decomposed; additionally, part of the inorganic impurities might be separated from the inner pore surface and removed from the diatomite pores. Some of the small impurities pieces could also be cleaned from the surface of the DU (panel b of Figure 1A). However, after HEEB irradiation at fluences of 10 and 20 kGy, the impurities in the pores as well as on the inner pore surface might become numerous loose pieces, which still existed in the pores, resulting in the decrease of the pore number (>120 nm) and increase of the Brunauer-Emmett-

dx.doi.org/10.1021/jf401274y | J. Agric. Food Chem. 2013, 61, 5215–5219

Teller (BET) surface area, as shown in curves a−c of Figure 1B and Figure 1C, compared to ND. When the HEEB fluence increased to 30 and 40 kGy, most of the loose impurity pieces were removed from the pores and a few piece of impurity could be seen on the diatomite surface (panels d and e of Figure 1A). That was to say, the amount of unclogged pores with a higher size increased, displaying an increase of the pore number (>140 nm) (curves d and e of Figure 1B) and a decrease of the BET surface area (BSA) (Figure 1C). From the pore structure investigation above, a conclusion could be obtained that HEEB was able to effectively modify the pore structure through removal of the impurities. Moreover, the modification effect increased with the increasing HEEB fluence.

X-ray diffraction (XRD) was performed to investigate the crystal structure of diatomite before and after HEEB treatment. As seen in the XRD spectra (Figure 2), no obvious new peak or

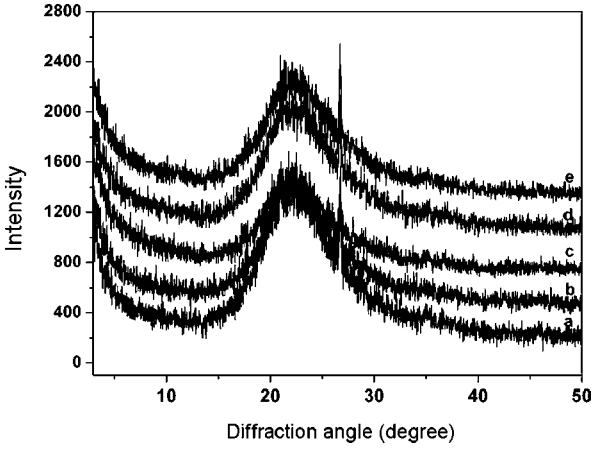

Figure 2. XRD spectra of (a) ND, (b) HMD10, (c) HMD20, (d) HMD30, and (e) HMD40.

peak shift was found, indicating that no new substance was generated and no obvious chemical reaction occurred during the HEEB irradiation process. In other words, this treatment was mainly originated from physical modification. With the increase of fluence, the characteristic peaks became weakened at first (≤20 kGy) while enhanced thereafter, illustrating that the order degree of diatomite decreased initially (≤20 kGy) and increased afterward. This was probably because HEEB irradiation made the impurities loose at fluences of 10 and 20 kGy, resulting in a lower order degree, while removing them out of the pores at fluences of 30 and 40 kGy, making the order degree increase again. This result agreed with the preceding pore structure analysis by SEM, PSD, and BSA. That was to say, HEEB could effectively modify the crystal structure of diatomite through mainly a physical process.

Interaction Analysis Between HMD and CPF. To investigate the interaction between HMD and CPF, the morphology of LCC was observed, as shown in Figure 3, which indicated that much more CPF could access the pores of HMD compared to ND. The number of pores filled with CPF increased with the electron beam fluence (almost all of the pores in HMD30 and HMD40 were filled with CPF), displaying that it was becoming easier for CPF to access the pores of HMD with increasing fluence. That was to say, the HMD treated with higher fluence possessed a higher adsorption capacity for CPF. This was because, with the increase of fluence, the impurities in pores were removed

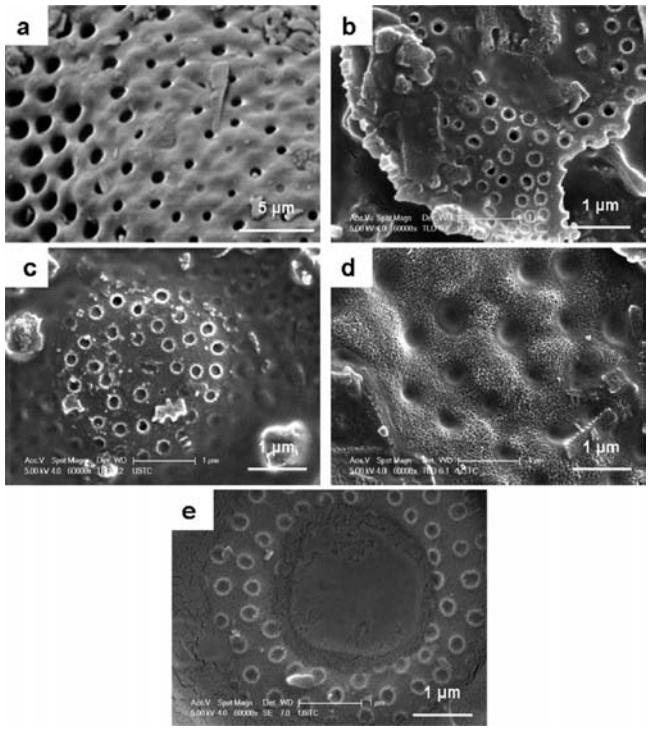

Figure 3. SEM images of (a) CPF0, (b) CPF10, (c) CPF20, (d) CPF30, and (e) CPF40.

gradually, which could facilitate the access of CPF. Furthermore, the amount of the hydrophilic groups (−OH, H_2O, etc.) on the inner surface of the pore might decrease because of the etching effect of HEEB, so that it was easier for the hydrophobic CPF to access.

FTIR measurement was also carried out, as illustrated in Figure 4. Peaks of both CPF (1542 cm^{-1} for C═N stretching

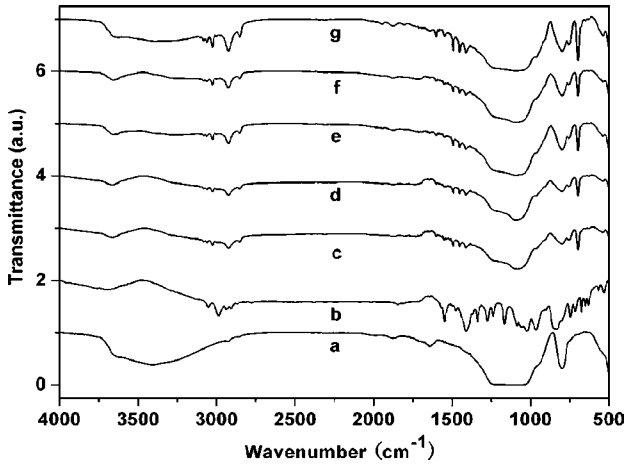

Figure 4. FTIR spectra of (a) ND, (b) CPF, (c) CPF0, (d) CPF10, (e) CPF20, (f) CPF30, and (g) CPF40.

vibration and 1412 cm^{-1} for pyridine stretching vibration) and diatomite (793 cm^{-1} for Si−O−Si stretching vibration) could be seen clearly in curves c−g of Figure 4, indicating that CPF was successfully adsorbed onto these diatomite samples. Moreover, the relative strength of the characteristic peaks of CPF (3039, 2917, 1542, and 1412 cm^{-1}) compared to that of diatomite (793 cm^{-1}) became higher with the increase of

dx.doi.org/10.1021/jf401274y | J. Agric. Food Chem. 2013, 61, 5215−5219

electron beam fluence. This demonstrated that the relative amount of CPF increased with the increasing fluence, which implied the HMD treated with a higher fluence owned a higher adsorption performance for CPF. In addition, the CPF peaks (3039 and 2978 cm^{-1}) (curve b of Figure 4) red-shifted to 3018 and 2917 cm^{-1} in LCC (curves c–g of Figure 4), which might be due to the formation of hydrogen bonds between CPF (–CH on the pyridine ring or $-CH_3$ in the branch chain) and diatomite (probably the Si–O–Si). Conclusionly, CPF could be more easily adsorbed onto HMD at higher fluence, and the interaction was probably the hydrogen bond.

Besides, the XRD patterns of LCC were investigated to obtain the crystal structure changes of HMD in LCC compared to ND. As shown in Figure 5, the main diffraction peaks of

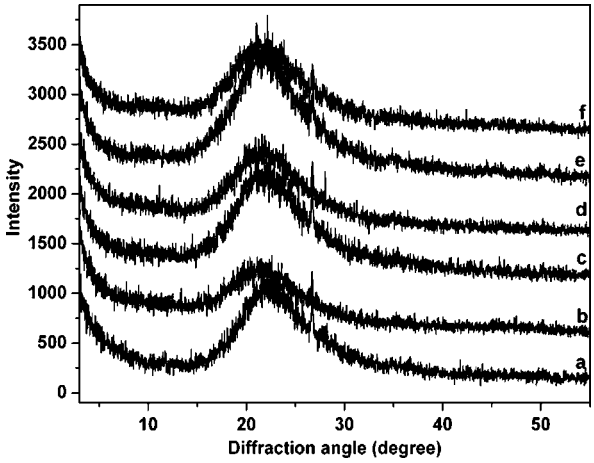

Figure 5. XRD spectra of (a) ND, (b) CPF0, (c) CPF10, (d) CPF20, (e) CPF30, and (f) CPF40.

these HMDs in LCC showed an obvious left shift compared to that of ND alone (22.3°), indicating that these HMDs in LCC possessed much higher layer distances than ND alone, which was probably due to the intercalation of CPF. Furthermore, the main diffraction peak of HMD in LCC gradually left shifted to 21.6° with the increasing fluence (0–40 kGy), which meant that the interlayer distance of HMD in LCC became higher with the increase of fluence, so that more and more CPF could access the crystal layers through the intercalation effect. From Figures 3 and 5, it could be concluded that CPF could be adsorbed onto HMD through access into both the pores and the crystal layers of diatomite.

Adhesion Performance of LCC on the Leaf Surface. Naturally, there were plenty of flower-like micro-nanosheets on the peanut leaf surface, clearly seen in panels A and B of Figure 6), making a rough surface and, thus, a high retaining ability for CPF (approximately 0.2 and 0.09 mg/leaf before and after washing). However, the retaining ability (or adhesion performance of CPF) was significantly enhanced for LCC containing HMD compared to CPF alone or CPF0 (Figure 6D), and CPF40 exhibited the highest retaining ability (approximately 0.44 and 0.18 mg/leaf before and after washing), which demonstrated that HMD could effectively improve the adhesion performance of CPF on the peanut leaf surface, resulting in a high anti-washing capacity and a low loss amount of CPF, so that the utilization efficiency of CPF increased and the utilization amount could be reduced. The significant increase of the adhesion performance of CPF was mainly attributed to the high adsorption and retaining capacities of

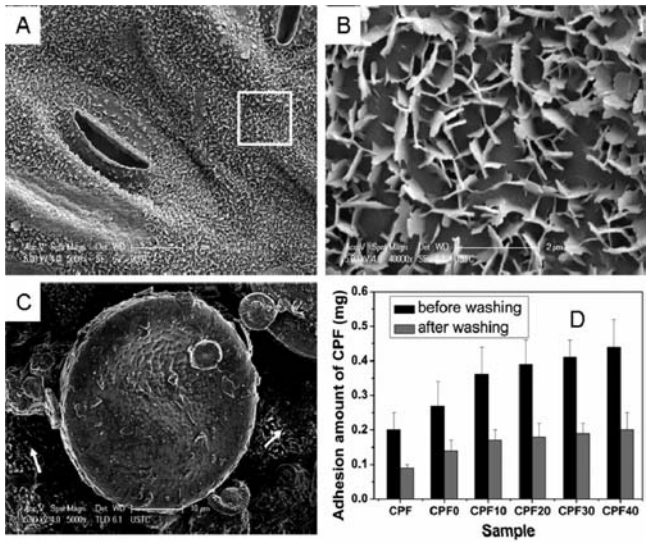

Figure 6. (A) SEM image of the peanut leaf surface (panel B is the magnification of the squared region in panel A), (C) SEM image of CPF40 on the peanut leaf surface, and (D) adhesion performance of different CPF samples.

HMD. The HMD loaded with CPF could be more prone to be retained by the micro-nanosheets on the peanut leaf surface; thus, CPF was difficult to wash off (Figure 6C). The higher fluence, the higher adsorption capacity of HMD and, thus, the higher adhesion performance of LCC. Therefore, by this means, the migration and loss of pesticide from the leaf surface of the crop could be controlled, which was favorable for reducing the environmental risk of pesticide.

Leaching Performance of LCC in Soil. HMD could not only increase the adhesion capacity of CPF on leaf surface but also reduce the leaching loss through the soil. As shown in Figure 7B, the leaching loss ratio of LCC based on HMD (10–40 kGy) could be decreased obviously compared to CPF alone and ND, which was due to the gradual increase of the adsorption ability of HMD for CPF. From Figure 7A, it could be seen that the HMD together with CPF was prone to be retained on the soil surface, making the soil surface much whiter compared to CPF alone. Obviously, the leaching loss of CPF reduced, and quite an amount of the CPF could be retained in the top layer of the soil, which was favorable for the photolysis and biolysis of CPF thereafter. Additionally, such migration control of pesticide in soil was beneficial for the protection of the groundwater.

In conclusion, in this paper, an approach for controlling CPF loss was developed using LCC prepared by adding HEEB-modified diatomite to CPF. HEEB treatment was proven to be an effective way to dredge the originally clogged pores in diatomite, making diatomite possess higher porosity and, meanwhile, creating a higher adsorption capacity for CPF, so that more CPF could be adsorbed in such a modified diatomite. Because of the high adsorption and retaining performance of HMD compared to CPF alone and ND, the resulting LCP displayed a significantly higher adhesion performance on the peanut leaf surface and a lower leaching loss ratio in the soil, which was beneficial to improve the utilization efficiency of pesticide and reduce the environmental risk of pesticide.

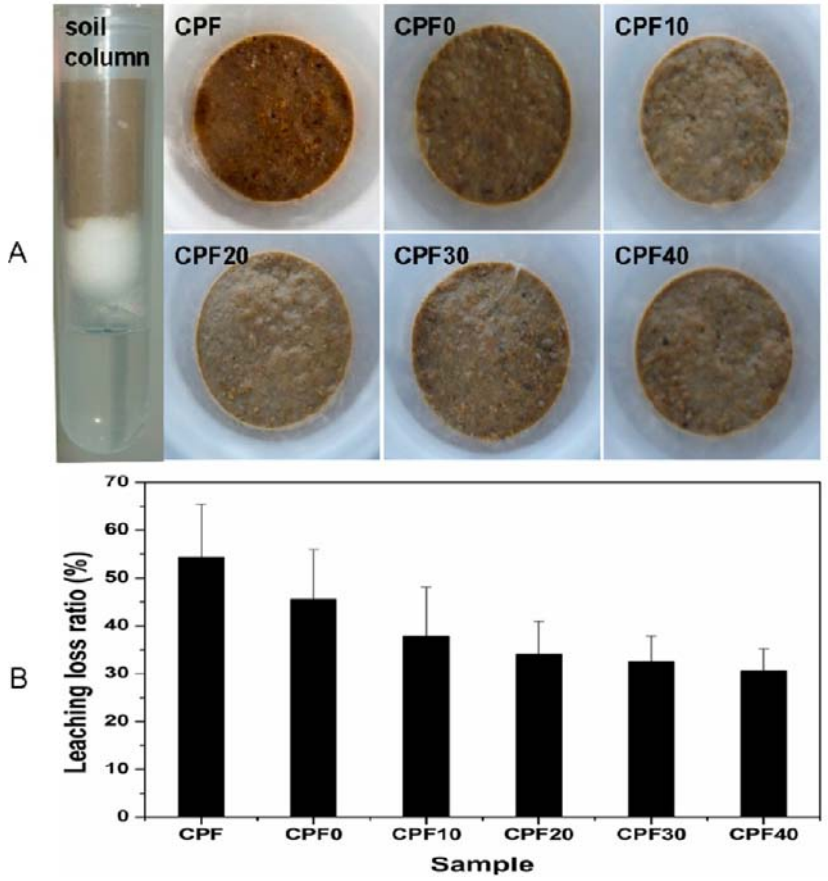

Figure 7. (A) Images of the soil column and the surface of soil after leaching for different CPF samples and (B) leaching loss ratio of different CPF samples.

AUTHOR INFORMATION

Corresponding Author

*Corresponding authors. Telephone: +86-551-65595012. Fax: +86-551-65591413. E-mail: dqcai@ipp.ac.cn (D.C.); zywu@ipp.ac.cn (Z.W.).

Funding

The authors acknowledge financial support from the National Natural Science Foundation of China (10975154) and the Scientific and Technological Project of Anhui Province (1206c0805014).

Notes

The authors declare no competing financial interest.

REFERENCES

(1) Gerstl, Z.; Nasser, A.; Mingelgrin, U. Controlled release of pesticides into soils from clay–polymer formulations. *J. Agric. Food Chem.* **1998**, *46*, 3797–3809.

(2) Gish, T. J.; Shirmohammadi, A.; Wienhold, B. J. Field scale mobility and persistence of commercial and starch encapsulated atrazine and alachlor. *J. Environ. Qual.* **1994**, *23*, 355–359.

(3) Vasilakoglou, B. I.; Eleftherohorinos, G. I. Activity, adsorption, mobility, efficacy and persistence of alachlor as influenced by formulation. *Weed Sci.* **1997**, *45*, 579–585.

(4) Gorski, F. S. Slow-release delivery system for herbicides in container-grown stock. *Weed Technol.* **1993**, *7*, 894–899.

(5) Johnson, R. M.; Pepperman, A. B. Leaching of alachlor from alginate-encapsulalated controlled release formulations. *Pestic. Sci.* **1996**, *48*, 157–164.

(6) Al-Degs, Y.; Khraisheh, M. A. M.; Tutunji, M. F. Sorption of lead ions on diatomite and manganese oxides modified. *Water Res.* **2001**, *35*, 3724–3728.

(7) Lemonas, J. F. Diatomite. *Am. Ceram. Soc. Bull.* **1997**, *76*, 92–95.

(8) Gao, B. G.; Jiang, P. F.; An, F. Q.; Zhao, S. Y.; Ge, Z. Studies on the surface modification of diatomite with polyethyleneimine and trapping effect of the modified diatomite for phenol. *Appl. Surf. Sci.* **2005**, *250*, 273–279.

(9) Zhang, G. L.; Cai, D. Q.; Wang, M.; Zhang, C. L.; Zhang, J.; Wu, Z. Y. Microstructural modification of diatomite by acid treatment, high-speed shear, and ultrasound. *Microporous Mesoporous Mater.* **2013**, *165*, 106–112.

(10) Grayston, S. J.; Wand, S.; Campbell, C. D.; Edwards, A. C. Selective influence of plant species on microbial diversity in the rhizosphere. *Soil Biol. Biochem.* **1998**, *30*, 369–378.

(11) Kale, S. P.; Carvalho, F. P.; Raghu, K.; Sherkhane, P. D.; Pandit, G. G.; MohanRao, A. Studies on degradation of ^{14}C-chlorpyrifos in the marine environment. *Chemosphere* **1999**, *39*, 969–976.

(12) Sundaram, B.; Rai, S. K.; Ravendra, N. Degradation of bifenthrin, chlorpyrifos and imidacloprid in soil and bedding materials at termiticidal application rates. *Pestic. Sci.* **1999**, *55*, 1222–1228.

(13) Subhani, A.; Liano, M.; Huang, C. Y.; Xie, Z. M. Impact of some agronomic practices on paddy field soil health under varied ecological condition: influence of soil moisture. *Pedosphere* **2001**, *11*, 38–48.

(14) Pandey, S.; Singh, D. K. Total bacterial and fungal population after chlorpyrifos and quinalphos treatments in groundnut (*Arachis hypogaea* L.) soil. *Chemosphere* **2004**, *55*, 197–205.

(15) Hebert, V. R.; Hoonhout, C.; Miller, G. C. Use of stable tracer studies to evaluate pesticide photolysis at elevated temperatures. *J. Agric. Food Chem.* **2000**, *48*, 1916–1921.